EUROPEAN COMMISSION

European Research Area

Long-term Performance of Engineered Barrier Systems

PEBS

Long-term Performance of Engineered Barrier Systems

PEBS

DELIVERABLE (D-N°:D3.5-2)

Formulation of a model suitable for long term predictions

Contract (grant agreement) number: ***FP7 249681***

Authors:

Antonio Gens (CIMNE-UPC), Marcelo Sánchez (Texas A&M)

Date of issue of this report: 02/05/14

Start date of project : **01/03/10** Duration : 48 Months

Project co-funded by the European Commission under the Seventh Euratom Framework Programme for Nuclear Research &Training Activities (2007-2011)		
Dissemination Level		
PU	Public	PU
RE	Restricted to a group specified by the partners of the PEBS project	
CO	Confidential, only for partners of the PEBS project	

EURATOM

TABLE OF CONTENT

1. INTRODUCTION

Engineered barriers will be subjected to thermal loads and hydromechanical phenomena over very long periods of time. In this context, the prediction of the likely long-term evolution of an engineered barrier in a repository is a significant challenge. Even in the case that a good representation of field test results has been achieved for the early stages of hydration and heating of a barrier (Sanchez et al., 2012), it is not a complete guarantee that such a good reproduction will continue in the long term. Indeed there have been a number of indications that conventional thermo-hydro-mechanical (THM) formulations exhibit significant shortcomings when dealing with long term simulations (Gatabin & Billaud, P., 2005; Thomas et al., 2003; Sanchez et al. 2012). This observation might indicate that the conventional formulation could be missing some relevant features or phenomena.

This fact is not surprising. It is certainly possible, and even likely, that phenomena that play a negligible role in the early stages of heating and hydration could become more relevant in the long term when the circumstances are quite different from those of early times. It should be expected, for instance, that hydraulic gradients inside the barrier will be much smaller at long times when the barrier is closer to saturation. In the repository, thermal gradients will also reduce with time but the rate at which they do so compared with that of the hydraulic gradients will depend on the specific features and geometry of the engineered barrier, the heating characteristics of the waste and to the properties of the host rock.

Engineered barriers are generally formed by compacted active clays in the form of blocks, powder, pellets or a combination of those. In all cases, the microfabric of the material (i.e. the arrangement of the basic structural elements: aggregates, pellets, clay particles and pores) will change very significantly over the course of heating and hydration of the barrier. Thus, the microfabric in the long term will be very different form the initial one. Naturally, such major variation of microfabric is bound to have a noticeable effect in the long term behaviour of the engineered barrier.

In this Deliverable, extensions to and modification of the conventional THM formulation to incorporate phenomena that could be relevant in the long term behaviour of engineered barriers are described. For completeness, the conventional THM formulation is introduced first. Afterwards, the modifications of the formulation to incorporate a number of phenomena are described. They are: non-Darcy flow, thermo-osmosis and microfabric evolution. Non-Darcy flow and thermo-osmosis are likely to be more relevant in the long term due to the smaller hydraulic gradients operating at the later stages. Also, after a long hydration period, microfabric changes will have had more time to accumulate thus becoming more significant.

2. CONVENTIONAL FORMULATION

2.1 General

The formulation of the conventional models is based on a macroscopic approach developed in the context of the continuum theory for porous media (Olivella et al., 1994; Gens, 2010). It is assumed that the porous medium is made up of three phases: solid, liquid and gas. The liquid phase contains water and dissolved air whereas the gas phase is made up of dry air and water vapour. The formulation incorporates basic thermal, hydraulic and mechanical phenomena in a coupled manner. The hydraulic component should be understood in a generalized way, i.e. including both liquid and gas flow.

In this Section the main parts of the basic THM formulation are presented. Specifically the basic THM formulation takes into account the following phenomena:

- Heat transport:
    - Heat conduction.
    - Heat convection (liquid water).
    - Heat convection (water vapour).
    - Phase changes
- Water flow:
    - Liquid phase.
    - Water vapour diffusion.
- Air flow:
    - Gas phase.
    - Air solution in water.
    - Dissolved air diffusion.
- Mechanical behaviour:
    - Thermal expansion of materials.
    - Generalized mechanical behaviour of materials dependent on stresses, suction, water pressure and temperature.

The problem is approached using a multi-phase, multi-species formulation that expresses mathematically the main *THM* phenomena in terms of:

- Balance equations.
- Constitutive equations.
- Equilibrium restrictions
- Phase physical properties

In the following Sections the main aspects of these four main parts of the basic formulation are presented.

2.2 Balance equations

The compositional approach has been adopted to establish the mass balance equations. This approach consists of balancing the species (mineral, water and air) rather than the phases (solid, liquid and gas). In this way the phase change terms do not appear explicitly, which is particularly useful when equilibrium is assumed. In the notation, the subscript is used to identify the phase (*s* for solid, *l* for liquid and *g* for gas) and the superscript indicates the species: *w* for water and *a* for air. No symbol is attributed to the mineral species, because it has been assumed that it coincides with the solid phase. The main balance equations are presented in the following paragraphs, a more detailed description can be found elsewhere (i.e. Olivella et al., 1994).

2.2.1 *Balance of mass of water:*

$$\frac{\partial}{\partial t}\left(\theta_l^w S_l \phi + \theta_g^w S_g \phi\right) + \nabla.\left(\mathbf{j}_l^w + \mathbf{j}_g^w\right) = f^w \qquad (1)$$

where θ_l^w and θ_g^w are the masses of water per unit volume of liquid and gas phase respectively. ϕ is the porosity and S_α is the volumetric fraction of pore volume occupied by the alpha phase (α=*l*,*g*). $\mathbf{j}_l^w$ and $\mathbf{j}_g^w$ denote the total mass fluxes of water in the liquid and gas phases with respect to a fixed reference system. f^w is the external mass supply of water per unit volume of medium.

2.2.2 *Balance of mass of air:*

$$\frac{\partial}{\partial t}\left(\theta_l^a S_l \phi + \theta_g^a S_g \phi\right) + \nabla.\left(\mathbf{j}_l^a + \mathbf{j}_g^a\right) = f^a \qquad (2)$$

where θ_l^a and θ_g^a are the masses of air per unit volume of liquid and gas phase respectively. $\mathbf{j}_l^a$ and $\mathbf{j}_g^a$ denote the total mass fluxes of air in the liquid and gas phases with respect to a fixed reference system. f^a is the external mass supply of air per unit volume of medium. Note that dry air is considered as a single species in spite of the fact that it is a mixture of gasses. The gaseous phase is assumed as a mixture of air and water vapour. Air is also dissolved in the liquid phase.

2.2.3 *Balance of energy:*

$$\frac{\partial}{\partial t}\left[E_s \rho_s \left(1-\phi\right)\right] + \frac{\partial}{\partial t}\left(E_l \rho_l S_l \phi + E_g \rho_g S_g \phi\right) + \nabla.\left(\mathbf{i}_c + \mathbf{j}_{Es} + \mathbf{j}_{El} + \mathbf{j}_{Eg}\right) = f^E \qquad (3)$$

The balance of energy has been expressed in terms of internal energy where E_s is the solid specific internal energy, E_l and E_g are specific internal energies corresponding to the liquid and gas phases respectively. ρ_l and ρ_g are the liquid and gas phase densities of the medium. f^E is the energy supply per unit volume of medium. The most important processes for energy transfer in a porous medium have been considered in (3), which are: conduction, advection and phase change. $\mathbf{i}_c$ is the conductive heat flux. $\mathbf{j}_s$, $\mathbf{j}_{El}$ and $\mathbf{j}_{Eg}$ are the energy fluxes due to the motion of phase. In this approach a thermal equilibrium between the phases has been assumed, therefore the temperature is the same for the phases and only one equation of total energy is required. This assumption is generally valid in low permeability media.

2.2.4 *Balance of mass of solid:*

$$\frac{\partial}{\partial t}\left(\rho_s \left(1-\phi\right)\right) + \nabla \cdot \left(\rho_s \left(1-\phi\right) \dot{\mathbf{u}}\right) = 0 \qquad (4)$$

where $\dot{\mathbf{u}}$ is the solid velocity vector. The variation of porosities in terms of changes in solid density and volumetric deformation of the soil skeleton is obtained from (4).

2.2.5 *Balance of momentum (equilibrium):*

$$\nabla.\boldsymbol{\sigma}_t + \mathbf{b} = 0 \tag{5}$$

where $\boldsymbol{\sigma}_t$ is the total stress tensor and **b** the vector of body forces. In (5) inertial terms have been neglected. This assumption is usually accepted because both velocities and accelerations are small, yielding terms that are negligible in comparison with the stress terms. The assumption of small strain rate is also made. Through an adequate constitutive model, the equilibrium equation is transformed into a form expressed in terms of the solid velocities, fluid pressures and temperatures.

2.3 Constitutive equations

The constitutive equations establish the link between the unknowns and the dependent variables. There are several categories of dependent variables depending on the complexity with which they are related to the unknowns. The governing equations are finally written in terms of the unknowns when the constitutive equations are substituted in the balance equations. Here, some of the basic constitutive laws are presented, divided in thermal, hydraulic and mechanical. In spite of this distinction between the three basic components of the problem, the constitutive equation provides in fact the links that couple the various phenomena considered in the formulation. The general expressions of the constitutive laws for the thermal, hydraulic and mechanical problems are presented below.

2.3.1 *Thermal*

Conductive heat flow is assumed to be governed by Fourier's law:

$$\mathbf{i}_c = -\lambda \nabla T \tag{6}$$

where λ is the global thermal conductivity of the porous medium, generally dependent on degree of saturation and porosity. A general expression, based on the geometric mean of the thermal conductivities of the three phases can be expressed as:

$$\lambda = \lambda_{sat}^{S_l} \lambda_{dry}^{(1-S_l)} \tag{7}$$

The internal energy for the medium is computed assuming that it is additive in relation to the phases (Olivella et al., 1994). Therefore, the following expression has been used:

$$E = E_s \rho_s \left(1-\phi\right) + E_l \rho_l S_l \phi + E_g \rho_g S_g \phi \tag{8}$$

where E_s, E_l and E_g are the specific internal energies corresponding to each phase, i.e., the internal energy per unit mass of phase. ρ_s, ρ_l, ρ_g, are the densities of the three phases, ϕ is the porosity and S_g is the gas fraction with respect to the pore volume.

The gas phase energy is generally expressed as:

$$E_g \rho_g = \left(E_g^w \omega_g^w + E_g^a \omega_g^a\right) \rho_g = E_g^w \theta_g^w + E_g^a \theta_g^a \tag{9}$$

where E^w_g and E^a_g are the specific internal energies of species (respectively water and air), that is, internal energy per unit of mass of species. ω^w_g and ω^a_g are the mass fraction of water and air species in gas phase, respectively. This additive decomposition is admissible for the gaseous phase in the assumption of a mixture of gasses. It is not so obvious that the same decomposition is also valid for the liquid phase, however the same assumption will be made since the significance of the internal energy of dissolved air is small:

$$E_l \rho_l = \left(E_l^w \omega_l^w + E_g^a \omega_l^a \right) \rho_l = E_l^w \theta_l^w + E_g^a \theta_l^a \tag{10}$$

The values of the specific internal energies for the individual species are (Batchelor, 1983; and Pollock, 1983): E^w_l =4180.0 (T-T_0) J/kg; E^w_g =2.5e^6+1900.0 (T-T_0) J/kg; E^a_g =1006.0 (T-T_0) J/kg and E^a_g =1006.0 (T-T_0) J/kg.

It can be noted that the specific internal energy of the vapour (water in gas phase) contains an additional term that represents the latent heat in vapour. The thermal consequences of evaporation/condensation are therefore taken into account in a straightforward way.

Finally, the law reported in Villar & Cuevas (1996) has been adopted for the internal energy per unit mass of solid phase. This expression is given by:

$$E_s = E_s^o T + c_p T^2 \tag{11}$$

2.3.2 *Hydraulic*

Advective phase fluxes (both liquid and water) are computed using generalized Darcy's law, expressed as:

$$\mathbf{q}_\alpha = -\mathbf{K}_\alpha \left(\nabla P_\alpha - \rho_\alpha \mathbf{g} \right); \qquad \alpha = l, g \tag{12}$$

where P_α is the phase pressure, $\mathbf{K}_\alpha$ is the permeability tensor of α phase and $\mathbf{g}$ is the gravity vector. The permeability tensor is not constant and depends on other variables, according to:

$$\mathbf{K}_\alpha = \mathbf{k} \frac{k_{r\alpha}}{\mu_\alpha}; \qquad \alpha = l, g \tag{13}$$

where $\mathbf{k}$ is the intrinsic permeability tensor, μ_α is the dynamic viscosity of the α phase and $k_{r\alpha}$ is the α phase relative permeability. The dependence of intrinsic permeability on pore structure is considered in terms of total porosity according to:

$$\mathbf{k} = k_0 \frac{\phi^3}{(1-\phi)^2} \frac{(1-\phi_0)^2}{\phi_0^3} \mathbf{I} \tag{4}$$

where k_0 is the reference permeability at the reference porosity ϕ_0.

The relative permeability of the liquid phase (k_{rl}) is made dependent on the degree of saturation according to:

$$k_{rl} = S_{el}^{\ n} \tag{85}$$

where n is a model parameter and S_{el} the effective degree of saturation, evaluated as follows:

$$S_{el} = \frac{S_l - S_{lr}}{S_{ls} - S_{lr}} \tag{16}$$

where S_{lr} is the residual saturation and S_{ls} is the maximum saturation. The relative permeability of the gaseous phase (k_{rg}) is obtained as follows:

$$k_{rg} = A S_g^{n_g} \tag{17}$$

where A and n_g are model parameters.

The retention curve adopted in the conventional formulation is based on the one proposed by van Genuchten (1978). The relation between degree of saturation and suction is given by:

$$S_{el} = \left[1 + \left(\frac{s}{P_o} \right)^{\frac{1}{1-\lambda_o}} \right]^{-\lambda_o} f_d \tag{18}$$

where P_o and λ_o are model parameters and f_d is a function included in order to model properly the high suction range where. The adopted expression is the following:

$$f_d = \left(1 - \frac{s}{P_d} \right)^{\lambda_d} \tag{19}$$

where P_d is related with the suction at 0 degree of saturation and λ_d is a model parameter. When $\lambda_d = 0$ the original model is recovered (Gens et al., 1998).

Non-advective fluxes of species inside the fluid phases are computed through Fick's law, which expresses them in terms of gradients of mass fraction of species through a hydrodynamic dispersion tensor that includes both molecular diffusion and mechanical dispersion:

$$\mathbf{i}_\alpha^i = -\mathbf{D}_\alpha^i \nabla \omega_\alpha^i; \qquad i = w, a; \qquad \alpha = l, g \tag{20}$$

where $\mathbf{D}^i_\alpha$ is the dispersion tensor of the medium. For vapour diffusion, the following expression for the hydrodynamic dispersion tensor is adopted:

$$\mathbf{i}_g^w = -\mathbf{D}_g^w \nabla \omega_g^w = -\left(\phi \rho_g S_g \tau D_m^w \mathbf{I} + \rho_g \mathbf{D}'_g \right) \nabla \omega_g^w \tag{21}$$

where D_m^w is the dispersion coefficient corresponding to molecular diffusion of vapour in air, $\mathbf{D}'_g$ is the mechanical dispersion tensor and τ is the tortuosity. Tortuosity takes into account the fact that the vapour diffusion takes place inside the voids of a porous media. The molecular diffusion coefficient is given by:

$$D_m^w = 5.9 x 10^{-12} \frac{\left(273.15 + T \right)^{2.3}}{P_g} \tag{22}$$

where D_m^w is in m^2/s, P_g is in MPa and T in ºC. It can be noted that in vapour diffusion, the THM couplings are evident: thermal effects through the variation of molecular diffusion with temperature; hydraulic effect through the influence of degree of saturation; and mechanical effects due to porosity changes. In the simulations it has been assumed that the molecular diffusion is dominant and the mechanical dispersion of vapour has been neglected. The same consideration can be made regarding diffusion of air in the liquid phase:

$$\mathbf{i}_l^a = -\mathbf{D}_l^a \nabla \omega_l^a = -\left(\phi \rho_l S_l \tau D_m^a \mathbf{I} + \rho_l \mathbf{D}'_l \right) \nabla \omega_l^a \tag{23}$$

2.3.3 *Mechanical*

A constitutive equation showing explicitly the contributions of strains, temperature and fluid pressures can be expressed generically as:

$$\dot{\boldsymbol{\sigma}} = \mathbf{D} \dot{\boldsymbol{\varepsilon}} + \mathbf{f} \dot{s} + \mathbf{t} \dot{T} \tag{24}$$

where $\boldsymbol{\sigma}$ is the constitutive stress (net or effective stress), $\boldsymbol{\varepsilon}$ is the strain vector, s is the matric suction computed as the difference between gas pressure and liquid pressure (p_g- p_l), **D** is the constitutive stiffness matrix, **f** is the generic constitutive vectors relating the changes in the fluid pressures and stresses and **t** is the constitutive vector relating stresses and temperature.

The Barcelona Basic Model, BBM, has been selected as the basis for the thermoplastic constitutive law in the conventional formulation. The BBM considers two independent stress variables to model the unsaturated behaviour: the net stress ($\boldsymbol{\sigma}$), computed as the excess of the total stresses over the gas pressure ($\boldsymbol{\sigma}_t$-$\mathbf{I}p_g$), and the matric suction (s). The BBM is an elasto-plastic model in which the yield surface depends not only on stresses (and history variables) but also on matric suction and temperature. A detailed description of the Barcelona Basic Model (BBM) model can be found in Alonso et al., (1990) and Gens (1995).

The BBM yield surface (F_{LC}) is expressed as follows:

$$F_{LC} = 3J^2 - \left[\frac{g(\theta)}{g(-30^o)}\right]^2 M^2 (p + p_s)(p_0 - p) = 0 \tag{25}$$

where p is the mean net stress, J is the square root of the second invariant of deviatoric stress tensor, M is the slope of the critical state, p_o is the apparent unsaturated pre-consolidation pressure, $g(\theta)$ is a function of the Lode angle (θ) and p_s considers the dependence of shear strength on suction and temperature.

The stress invariants are defined as:

$$p = \frac{1}{3}(\sigma_x + \sigma_y + \sigma_z) \tag{26}$$

$$J^2 = 0.5 \ \text{trace}(\mathbf{s}^2) \tag{27}$$

$$\theta = -\frac{1}{3}\sin^{-1}(1.5\sqrt{3}\ \det \mathbf{s}/J^3) \tag{28}$$

$$\mathbf{s} = \boldsymbol{\sigma} - p\mathbf{I} \tag{29}$$

$$\boldsymbol{\sigma} = \boldsymbol{\sigma}_t - \mathbf{I}p_f \tag{30}$$

where:

$$p_f = p_g \quad if \quad p_g > p_l \ ; \qquad \text{otherwise} \qquad p_f = p_l \tag{31}$$

$\boldsymbol{\sigma}_t$ is the total stress vector and **I** is the identity tensor.

The dependence of shear strength on suction and temperature is expressed as:

$$p_s = -k_s e^{-\rho \Delta T} \tag{32}$$

where k and ρ are model parameters and ΔT is the temperature increment, respect to the reference temperature T_o.

The equation that defines the set of yield p_0 values for the associated suction (i.e. the family of *LC* curves on a *p*-*s* plane) is given by:

$$p_0 = p_c \left(\frac{p_{0T}^*}{p_c} \right)^{\frac{\lambda_{(0)} - \kappa}{\lambda_{(s)} - \kappa}} \tag{33}$$

where p_c is a reference stress, κ is the elastic stiffness parameter for changes in net mean stress, p_{0T}^* is the pre-consolidation net mean stress for saturated conditions and current temperature. $\lambda_{(s)}$ is the compressibility parameter for changes in net mean stress for virgin states of the soil, the dependence of which with respect to the suction is expressed as:

$$\lambda_{(s)} = \lambda_{(0)} \left[r + (1 - r) e^{-\zeta s} \right] \tag{34}$$

where r is a parameter that defines the maximum soil stiffness and ζ is the parameter that controls the rate of increase of soil stiffness with suction.

In order to identify a single yield curve from (A.7), it is necessary to specify the pre-consolidation net stress for saturated conditions p_{0T}^*, which may be viewed as the hardening parameter of the BBM model. According to Gens (1995), the thermal effect has been included considering a dependence of the hardening parameter on temperature, as follows:

$$p_{0T}^* = p_0^* + 2\left(\alpha_1 \Delta T + \alpha_3 \Delta T \left| \Delta T \right| \right) \tag{35}$$

where α_1 and α_3 are model parameters.

The plastic potential (G) is expressed as:

$$G = \alpha 3J^2 - \left[\frac{g(\theta)}{g(-30^o)} \right]^2 M^2 \left(p + p_s \right)\left(p_0 - p \right) = 0 \tag{36}$$

where α is determined from the condition that the flow rule predicts zero lateral strains in a K_0 stress path (Alonso et al., 1990).

The hardening law is expressed as a rate relation between the volumetric plastic strain (ε_v^p) and the saturated isotropic pre-consolidation stress (p^*_0), according to:

$$\dot{p}_0^* = \frac{(1 + e)}{(\lambda_{(0)} - \kappa)} p_0^* \dot{\varepsilon}_v^p \tag{37}$$

where e is void index, κ is the elastic stiffness parameter for changes in net mean stress and $\lambda_{(0)}$ is the compressibility parameter for changes in net mean stress for virgin states of the soil in saturated conditions.

The expressions of the elasto-plastic tensors that define the small strain-stress relations are presented in Sánchez (2004) and Sánchez et al. (2005). Here only the elastic tensor is presented, which is evaluated as follows:

$$\mathbf{D}_e = \begin{bmatrix} K+\frac{4}{3}G_t & K-\frac{2}{3}G_t & K-\frac{2}{3}G_t & 0 & 0 & 0 \\ & K+\frac{4}{3}G_t & K-\frac{2}{3}G_t & 0 & 0 & 0 \\ & & K+\frac{4}{3}G_t & 0 & 0 & 0 \\ & & & G_t & 0 & 0 \\ symm & & & & G_t & 0 \\ & & & & & G_t \end{bmatrix} \tag{38}$$

where K is the global bulk modulus and G_t is the shear modulus. The macrostructural bulk modulus for changes in mean stress is computed as:

$$K = \frac{(1+e)}{\kappa} p \tag{39}$$

The shear modulus G_t can be obtained from a linear elastic model with constant Poisson's coefficient:

$$G_t = \frac{3(1-2\mu)K}{2(1+\mu)} \tag{40}$$

where μ is the Poisson's coefficient.

The macrostructural bulk modulus for changes in suction has been computed considering the following law:

$$K_s = \frac{(1+e)(s+p_{atm})}{\kappa_s} \tag{41}$$

Finally the macrostructural bulk modulus for changes in temperature is evaluated through the expression (Gens, 1995):

$$K_T = \frac{1}{(\alpha_0 + 2\alpha_2 \Delta T)} \tag{42}$$

A relevant aspect to comment here is that the original BBM is not able to reproduce satisfactorily the swelling behaviour of clays. Therefore, some modifications in the elastic part of the model are introduced in order to reproduce the expansive behaviour of bentonites. This is required mainly because the description of the material behaviour inside the yield surface is particularly important due to the high compaction that the bentonite blocks have been subjected to. The variation of stress-stiffness with suction and, especially, the variation of swelling potential with stress and suction have been considered. The resulting elastic model is the following:

$$\dot{\varepsilon}_v^e = \frac{\kappa}{(1+e)}\frac{\dot{p}}{p} + \frac{\kappa_s}{(1+e)}\frac{\dot{s}}{(s+p_{at})} + (\alpha_0 + \alpha_2 \Delta T)\dot{T} \tag{43}$$

$$\dot{\varepsilon}_s^e = \frac{\dot{J}}{G_t} \tag{44}$$

where ε_v^e and ε_s^e are the volumetric and deviatoric component of the elastic strain, respectively. κ_s is the elastic stiffness parameter for changes in suction; α_0 and α_2 are model parameters. ΔT is the temperature difference with respect to an arbitrary reference temperature T_0. G_t is the shear modulus, obtained from a linear elastic model.

The following expression has been proposed to evaluate the elastic stiffness parameter for changes in net mean stress:

$$\kappa = \kappa_0 \left(1 + \alpha_s s\right) \tag{45}$$

where κ_0 is the elastic stiffness parameter in saturated conditions and α_s is a model parameter. The elastic stiffness parameter for changes in suction is computed according to:

$$\kappa_s = \kappa_{s0} \left(1 + \alpha_{sp} \ln p / p_{ref}\right) \tag{46}$$

where κ_{s0} and α_{sp} are model parameters.

2.4 Equilibrium restrictions

It is assumed that phase changes are rapid in relation to other characteristic times typical of the problem under consideration. Therefore, they can be considered to be in local equilibrium, giving rise to a set of equilibrium restrictions that must be satisfied at all times. Equilibrium restrictions are given for the concentration of water vapour in gas phase and for the concentration of dissolved air in liquid phase.

The vapour concentration in the gaseous phase is governed by the psychometric law, which can be expressed as:

$$\theta_g^w = \left(\theta_g^w\right)^0 \exp\left(\frac{\Psi M_w}{R\left(273.15 + T\right)\rho_l}\right) \tag{47}$$

where θ_g^w is the vapour concentration in the gas phase; $(\theta_g^w)^0$ is the vapour concentration in the gas phase in equilibrium with a liquid at flat surface (at the sample temperature). Ψ is the total water potential of the water (excluding gravity terms); M_w is the molecular mass of the water (0.018 kg/mol) and R the gas constant (8.314 J/mol/ºK).

Henry's law is adopted to define the amount of air dissolved in water. This law expresses a linear relationship between the concentration of air in dissolution and the partial pressure of air (P_a) in the gaseous phase:

$$\theta_l^a = \omega_a^l \rho_l = \frac{P_a}{H} \frac{M_a}{M_w} \rho_l \tag{48}$$

where M_a is the molecular mass of the air (0.02895 kg/mol), and H is Henry's constant (1000 MPa).

2.5 Phase physical properties

The properties of the fluid phase appear in the balance equations and in the constitutive laws. In general, they depend on the composition of the phase and on the state variables (temperatures and pressures).

The function of density for the liquid phase can be expressed as (i.e. Olivella, 1995 and Gens & Olivella, 2001):

$$\rho_l = 1002.6 \exp\left(4.5x10^{-4}\left(P_l - 0.1\right) - 3.4x10^{-4}T\right) \tag{49}$$

where T is expressed in ºC, P_l in MPa and in ρ_l kg/m^3. This expression must have a cut-off for large negative liquid pressures; if not, unrealistic low liquid density is obtained.

The air density is obtained from the law of ideal gases:

$$\theta_g^a = \frac{M_a P_a}{R\left(273.15 + T\right)} \tag{50}$$

The density of the gas phase is obtained adding the partial densities of the two species:

$$\rho_g = \theta_g^w + \theta_g^a \tag{51}$$

Finally, the viscosity of the liquid and gas phase are, respectively (Olivella, 1995):

$$\mu_l = 2.1x10^{-12} \exp\left(\frac{1808.5}{273.15 + T}\right) \tag{52}$$

$$\mu_g = 1.48x10^{-12} \exp\left(\frac{\left(273.15 + T\right)^{1/2}}{1 + \frac{119}{\left(273.15 + T\right)}}\right) \tag{53}$$

where T is expressed in ºC and μ_α in MPa.s.

2.6 Computer code

The formulation outlined above has been implemented in the computer code CODE_BRIGHT (Olivella et al., 1996; CODE_BRIGHT User's Manual, 2014). It is a finite element code designed to solve thermo-hydro-mechanical problems in geological media. One unknown (state variable) is associated with each of the balance equations presented. The unknowns are obtained by solving the system of PDE's (Partial Differential Equations) numerically in a coupled way.

The state variables are: solid velocity, **u** (one, two or three spatial directions); liquid pressure, P_l; gas pressure, P_g ; and temperature T. From state variables, dependent variables are calculated using the constitutive equations or the equilibrium restrictions. Strains are defined in terms of displacements. Small strains and small strain rates are assumed for solid deformation. Advective terms due to solid displacement are neglected after the formulation is transformed in terms of material derivatives (in fact, material derivatives are approximated as eulerian time derivatives). The numerical approach can be viewed as divided in two parts: spatial and temporal discretization. Galerkin finite element method is used for the spatial discretization while finite differences are used for the temporal discretization. The discretization in time is linear and an implicit scheme is used. Finally, since the problem presented here is non-linear, the Newton-Raphson method was adopted as iterative scheme.

A feature of the numerical approach is that it can use a wide library of elements including segments, triangles, quadrilaterals, tetrahedrons, triangular prisms and quadrilateral prisms. Linear interpolation functions and, for some elements, quadratic interpolation functions are adopted. Analytical or numerical integration is used depending on element type. For the mechanical problem, selective integration is used for quadrilateral plane elements and quadrilateral prisms where the volumetric part is integrated with a reduced integration of 1 point.

The program has a scheme for the automatic discretization of time. Reduction of time increment may be caused by excessive variation of unknowns per iteration, by excessive number of iterations to reach convergence or if the correction is larger than in the previous iteration (more details in CODE_BRIGHT User's Manual, 2014). Convergence criteria are established in terms of forces or flows and of state variables. Regarding the boundary conditions of the mechanical problem, forces and displacement rate can be enforced in any spatial direction and at any node. In the hydraulic problem, mass flow rate of water and dry gas can be prescribed at any node, or liquid/gas pressure can be also enforced at any node. Finally, regarding the thermal problem, heat flow and temperature can be prescribed at any node of the mesh (Olivella et al., 1996; CODE_BRIGHT User's Manual, 2014).

The structure of the computer code has proved to be flexible enough to accommodate the modifications of the formulation described below.

3. MODIFIED FORMULATION FOR LONG TERM PREDICTIONS

As anticipated in the Introduction, the conventional formulation has been modified in order to take into account phenomena that may be significant for long term analyses. They are:

- Non-Darcy flow
- Thermo-osmosis.
- Microfabric evolution

Each of those modification is examined in the following sections.

3.1 Non-Darcy flow

This Section considers the possibility of a limit of applicability of the Darcy's law at low hydraulic gradients. Some experimental evidence shows that under low hydraulic gradients (J), Darcy's simple relationship does not govern the liquid flow in some porous media, especially in soils containing active clay minerals. Arguments based on the strong clay-water interactions have been suggested to explain this non-Darcian flow behaviour (*i.e.* Bear, 1972). Obviously, departures from Darcy's law only become evident at low hydraulic gradients that correspond to the long term situation when the barrier is close to full hydration.

There are several ways to describe this phenomenon. A well-known law considers two characteristic gradients (Figure 1): the threshold hydraulic gradient (J_o) and the critical hydraulic gradient (J_c). J_o is the hydraulic gradient below which no flow occurs. J_c is the hydraulic gradient below which flow occurs but it is not Darcian. If the hydraulic gradient is higher than J_c the proportionality between gradient increments and flow increments is recovered.

A certain amount of experimental work can be found in the literature exploring the validity of the Darcy's law under low gradient in saturated conditions (i.e. Hansbo, 1960; Russell & Swartzendruber, 1971; Dixon et al., 1992). A threshold gradient close to 50 has been reported in some of these works. This deviation from the Darcy's law is explained considering the high energy of the adsorbed water (Dixon et al., 1992, 1999; Cui et al., 2001) and also the pore clogging effect when active clays are present in the porous media (Russell & Swartzendruber, 1971; Cui et al., 2001). Cui et al. (2001) detected much higher values of critical gradient, close to 7500, in a pressure reduction path for a mixture of sodium bentonite and sand (in a proportion of 7/3 in mass).

When low permeability clays are tested, the main problem is the long time required by the experiments and the possibility of experimental error. An experimental technique to overcome these problems often used is the application of large hydraulic gradients. But then, the potential existence and values of the threshold gradients are harder to detect.

From the formulation point of view, the only change required is to modify the flow equation as:

$$\mathbf{q}_l = -\mathbf{K}_l\left(\nabla P_l - \rho_l \mathbf{g}\right) = -\frac{\mathbf{k}}{\mu_l}\left\langle \frac{J - J_o}{J} \right\rangle^{n_l} \left(\nabla P_l - \rho_l \mathbf{g}\right) \tag{54}$$

and

$$\mathbf{J} = \nabla\left(\frac{p}{\gamma_l} + z\right) \quad \text{and} \quad J = \left|\mathbf{J}\right| \tag{55}$$

where J_o is the threshold gradient and n_t is a parameter that controls the value of the critical gradient J_c.

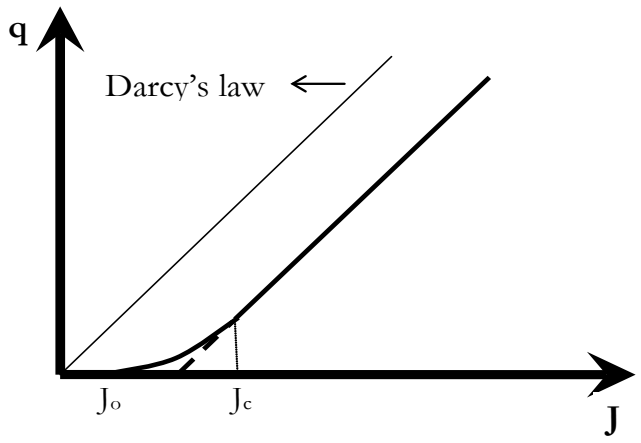

Figure 1. Schematic representation of the hydraulic threshold gradient (Dixon et al., 1992).

3.2 Thermo-osmosis

It is generally agreed that the hydraulic gradient is the main force influencing the movement of water in the soils. It is, however, not the only one. Figure 2 presents the different kinds of flow (apart from the electrical component) that can occur in the porous media and the corresponding gradient responsible for the movements. The word 'law' is used for the diagonal terms associated to the direct flow phenomena, and the name 'effect' is reserved for the non-diagonal ones, called 'coupled processes' (i.e. Bear, 1972; Mitchell, 1993). The Figure also includes the names given to some of these flows.

The 'phenomenological coefficient' that links each flow with the corresponding driving force must be measured experimentally (Mitchell, 1993). Generally, the non-diagonal coefficients are relatively small and negligible compared to the diagonal terms and the coupled process can be ignored. However there are certain problems in which, due to their particular conditions, the coupled process may play a more influential role.

This may occur, for instance, in non-isothermal problems involving very low permeability materials under low hydraulic gradients where the flow due to hydraulic driving forces may end up being comparable to the flow induced by temperature gradients; i.e. the thermo-osmotic effects may not be negligible. Low hydraulic gradients are of course more likely at long times, i.e in the later phases of hydration. To account for thermo-osmosis, a new term has to be added to the equation for liquid flow:

$$\mathbf{q}_l = -\mathbf{K}_l \left(\nabla P_l - \rho_l \mathbf{g} \right) - \mathbf{K}_{HT} \nabla T \qquad (56)$$

where $\mathbf{K}_{HT}$ is the thermo-osmotic coefficient.

Unfortunately, experimental evidence on the value of the thermo-osmotic coefficient is scarce or altogether lacking. Values falling in the very wide range of 10^{-10}-10^{-14} $m^2/K/s$ have been reported in the literature (Soler, 1999, 2001; Djeran, 1993).

Flow	Gradients		
	Hydraulic Head	**Chemical Concentration**	**Temperature**
Fluid	**Darcy's Law** (Hydraulic Conduction)	**Chemical Osmosis**	**Thermo Osmosis**
Solutes	**Ultra Filtration**	**Fick's Law** (Diffusion)	**Soret Effect** (Thermal Diffusion)
Heat	**Thermo Filtration** (Isothermal Heat Transfer)	**Dufour Effect**	**Fourier's Law** (Thermal Conduction)

Figure 2. Direct and coupled flow processes

3.3 Micro-fabric evolution

The fabric of a heavily compacted clay generally presents generally a very marked double structure character. It consists of dense aggregates of clay particles with intra-aggregate pores (micropores) between them. The arrangement of these clay aggregates conforms a granular skeleton of the material, with interaggregate pores (macropores) between them. Once hydration starts, the clay aggregates tend to adsorb water and swellIf the material is confined the expansion of the microstructure is made possible by reductions of the macropores. This has a significant influence on the permeability value and hence on the hydration of the barrier, especially in the long term when the microfabric changes are more advanced. These phenomena imply a dynamic character of the clay fabric during wetting, resulting in a strong coupling between the mechanical and the hydraulic problem.

Experimental evidence of the microfabric evolution can be obtained by direct observation using electron-microscopy techniques. Thus, for instance, Figure 3a shows a micrograph of a bentonite compacted under hygroscopic conditions to r_d=1.65 Mg/m^3 obtained using SEM where the presence of aggregates, the size of inter-aggregate voids and the bimodal distribution of pore sizes are readily apparent. Suction changes under isochoric conditions were the applied to specimens before subjecting them to microstructural observations. Figure 3b presents the image of the clay fabric after application of a suction of 10 MPa ($r_{d\ final}$=1.46 g/cm^3). Figure 3c shows the microstructure, after saturation under isochoric conditions ($r_{d\ final}$=1.43 g/cm^3), on bentonite initially compacted with hygroscopic water content to r_d=1.65 Mg/m^3. The differences in final dry density are due to the rebound experienced by the bentonite after unloading. The progressive occlusion of the inter-aggregate pores due to particle swelling can be easily noted. Although in an engineered barrier the overall porosity of the material will remain rather constant, it is obvious that the intrinsic permeability will reduce drastically as permeability depends more on pore size than on total porosity.

Additional experimental evidences of this strong hydro-mechanical behaviour can be found in Cui et al. (2001), in which measured values of macroporosity and permeability at different suctions are reported (Figure 4). As the water flow takes place predominately through the macropores, it is possible to suggest that changes in macroporosity could explain the reduction in the permeability at advanced stages of hydration.

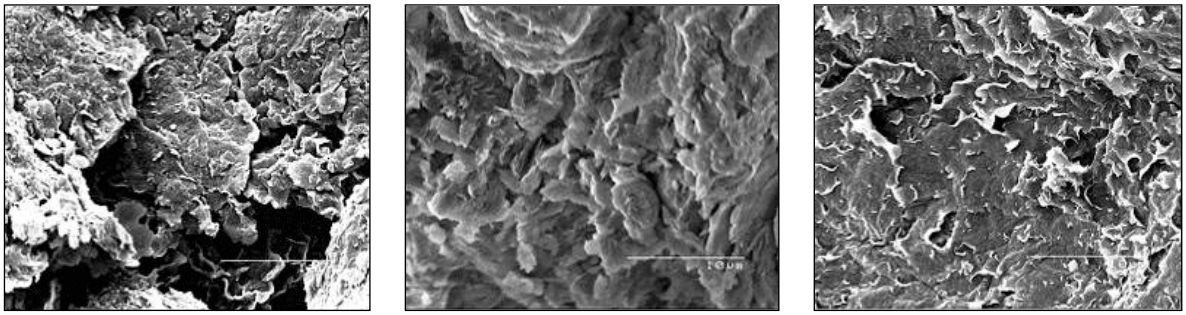

a) b) c)

Figure 3. Micrographs (SEM, x 6000). a) Compacted with hygroscopic water content to ρ_d=1.40 g/cm^3. b) After application of a suction of 10 MPa in isochoric conditions ($\rho_{d\ final}$=1.46 g/cm^3) on bentonite initially compacted in hygroscopic conditions to ρ_d=1.65 Mg/m^3 and c) after saturation in isochoric conditions (ρ_d final=1.43 g/cm^3) on bentonite initially compacted with hygroscopic water content to ρ_d=1.65 Mg/m^3 (FEBEX II Report, 2004).

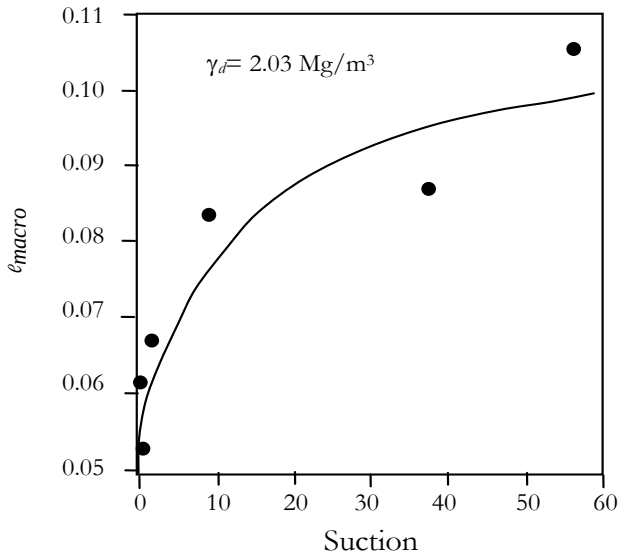

Figure 3. Variation of the macropores void ratio with suction (Cui et al., 2001).

In the case of barriers formed using pellet-based materials, the double structure is still more clearly apparent. The granular arrangement of the pellets constitutes the macrostructure whereas the microstructure corresponds to the material arrangement inside the pellets. Microfabric evolution will also be very relevant in those materials. Therefore, the constitutive model used to represent the barrier materials should be able to take into account the evolution of the microfabric.

For this purpose, a mechanical model for double structure expansive materials has been adopted. The model integrates the main aspects of expansive clay behaviour in a unified and formal framework. The mechanical law is based on the general approach proposed by Gens & Alonso (1992) and also considers some of the improvements proposed by Alonso et al. (1999). Particular attention is placed on clay structure and how it can be incorporated in the constitutive modelling of expansive soils.

The mechanical model has been developed using concepts of elasto-plasticity for strain hardening materials. The model is formulated in terms of three stress invariants (*p, J, q*), suction (*s*) and temperature (*T*), where *p* is the mean net stress, *J* is the square root of the second invariant of deviatoric stress tensor and *q* is Lode's angle. The expressions for the evaluation of the invariants have been given in section 2.3.3.

A characteristic of this model is the explicit consideration of the two main structural levels and also the interaction between the two structures. Therefore, the complete formulation of the model requires the definition of laws for describing the behaviour of:

- The macrostructural level.
- The microstructural level.
- The interaction between the structural levels.

Macrostructural model

The inclusion of this structural level in the analysis allows the consideration of phenomena that affect the skeleton of the material, for instance deformations due to loading and collapse. These phenomena have a strong influence on the macroscopic response of expansive materials. The macrostructural behaviour can be described by concepts and models of unsaturated non-expansive soils, such as the elasto-plastic Barcelona Basic Model (BBM) presented in Section 2.3.3. In the double structure model, constant values of k and k_s are assumed. Figure 5.a) presents a three dimensional representation of BBM in the space: *p, J, s.*

Microstructural model

The microstructure is associated with the active clay minerals, and its behaviour is controlled mainly by the physico-chemical phenomena occurring at this level. It is assumed that these phenomena are basically reversible. The strains arising from microstructural phenomena are considered elastic and volumetric. The microstructural effective stress is defined as:

$$\hat{p} = p + \chi s_t ; \qquad s_t = s_2 + s_o \tag{57}$$

where s_o the osmotic suction. Hydraulic equilibrium between the water potentials of both structural levels is assumed (this implies $s=s_1=s_2$). The extension of the constitutive model to handle problems in which this hypothesis is released is presented in Sanchez (2004).

In the *p-s* isotropic plane, the line corresponding to constant microstructural effective stresses is referred to as Neutral Line (*NL*), since no microstructural deformation occurs when the stress path moves on it (Figure 5.b). The increment of microstructural elastic strains is expressed as:

$$\dot{\varepsilon}_{v_1}^{e} = \frac{\dot{\hat{p}}}{K_1} = \frac{\dot{p}}{K_1} + \chi \frac{\dot{s}}{K_1} \tag{58}$$

where the subscript 1 refers to the microstructural level and the superscript *e* refers to the elastic component of the volumetric (subscript *v*) strains. For the microstructural bulk modulus (K_1) the following law has been adopted:

$$K_1 = \frac{e^{-\alpha_m \hat{p}}}{\beta_m} \tag{59}$$

where α_m and β_m are model parameters.

According to Figure 9.b) the Neutral Line divides the *p*-*s* plane into two parts (Figure 5b), identified as:

$\hat{p} > 0$ Þ microstructural contraction (*MC*) ; $\hat{p} < 0$ Þ microstructural swelling (*MS*)

Interaction between structural levels

In expansive soils there are other mechanisms in addition to the ones included in the BBM that induce plastic strains. This irreversible behaviour is attributed to the interaction between the macro and micro structures. Analysing the behaviour of expansive clays under cycles of suction reversals (e.g. Pousada, 1984), two main aspects can be highlighted: the irreversible behaviour appears independently of the applied suction and it is difficult to determine the initiation of yielding. These facts suggest the use of the more general framework of generalized plasticity theory to formulate the model. In a generalized plasticity model the yield function is not defined or, at least, it is not defined in an explicit way. This is particularly advantageous in expansive materials, because no clear evidence exists concerning the shape of the internal yield surfaces corresponding to the interaction mechanisms between the two structural levels (Sánchez et al., 2005).

It is assumed that the microstructural behaviour is not affected by the macrostructure but the opposite is not true, i.e. macrostructural behaviour can be affected by microstructural deformations, generally in an irreversible way. An assumption of the model is that the irreversible deformations of the macrostructure are proportional to the microstructural strains according to interaction functions *f*. The plastic macrostructural strains are evaluated by the following expression:

$$\dot{\varepsilon}^{p}_{v2} = f\,\dot{\varepsilon}^{e}_{v1} \qquad (60)$$

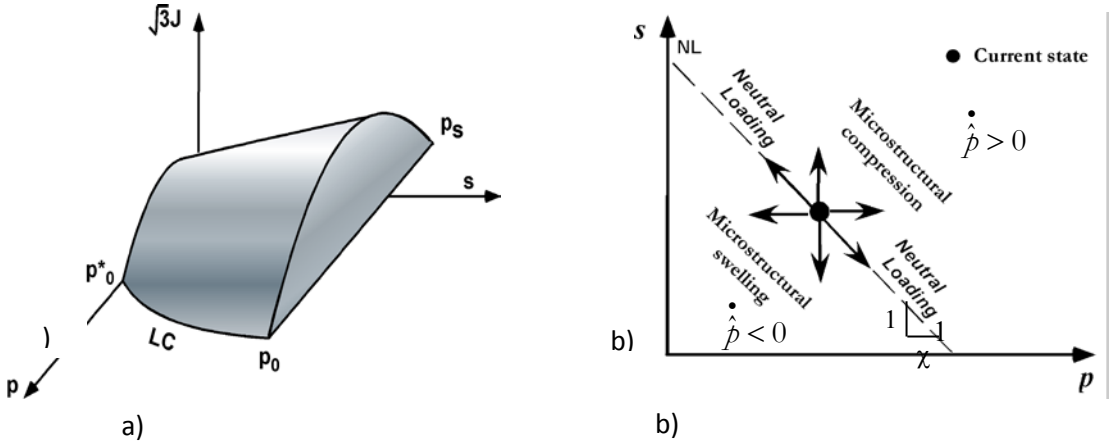

Figure 4. a) Three dimensional representation of the BBM yield surface. b) Definition of microstructural swelling and contraction directions.

Two interaction functions *f* are defined: f_c for microstructural contraction paths and f_S for microstructural swelling paths. In the case of isotropic load, the interaction function depends on the ratio p/p_o (p_o is the net mean yield stress at current suction and temperature). This ratio is a measure of the degree of openness of the macrostructure. When p/p_o is low it implies a dense packing of the material. It is expected that under this condition the microstructural swelling (*MS* path) affects strongly the global arrangements of clay aggregates. Therefore, the higher values of the f_s function correspond to low values of p/p_o. In this case the microstructure effects induce a more open macrostructure, which implies a macrostructural softening. On the other hand, when the microstructure contracts (*MC* path) the larger (induced) macrostructural plastic strains

occur with open macrostructures (values of p/p_o close to 1). Under this path the clay tends to a more dense state, which implies a hardening of the macrostructure. This coupling between both plastic mechanisms is considered mathematically assuming that:

$$\dot{\varepsilon}_v^p = \dot{\varepsilon}_{vLC}^p + f\,\dot{\varepsilon}_{v1}^e \tag{61}$$

where ε_{vLC}^p is the plastic strains induced by the yielding of the macrostructure (BBM). In fact the coupling is given by p_o^*, the hardening variable of the macrostructure (Figure 5.a), which depends on the total plastic volumetric strain (37). In this way the possibility that microstructural effects can affect the global arrangements of aggregates (macrostructure) is considered.

Note that the material response will depend strongly on the direction of the microstructural stress path relative to the *NL*, which delimits two regions of different material behaviour. A proper modelling of this behaviour requires the definition of specific elasto-plastic laws for each domain, in order to describe correctly the material behaviour according to the microstructural stress path followed (*MC* or *MS*). Generalized plasticity theory can deal with such conditions, allowing the consideration of two directions of different behaviour and the formulation of proper elasto-plastic laws for each region (Sánchez et al., 2005).

In summary, the behaviour of the macrostructure is modelled in the context of classical plasticity (BBM). This is a proper framework because the yield surface associated to this behaviour can be generally inferred using the usual methodology of classic plasticity. The microstructural effects have been modelled using a nonlinear elastic model. The interaction between both structural levels has been modelled using the more general framework of generalized plasticity theory. As described in Sánchez (2004) and Sánchez et al. (2005), the governing small strain-stress equations have been obtained using a general framework for multidissipative materials. Finally the numerical integration of the model has been performed using a scheme with error control.

As a consequence of using this double structure model, it is possible to track the values of the macroporosity and the microporosity at every stage of the hydration of the barrier. The effect of microfabric evolution on liquid flow is taken into account by assuming that the flow of liquid water takes place through the macropores. Consequently, the intrinsic permeability is a function of the macro porosity through the exponential law:

$$\mathbf{k} = k_0 \exp[b(\phi_M - \phi_{M0})]\mathbf{I} \tag{62}$$

where k_0 is the intrinsic permeability at the reference macroporosity ϕ_{M0}, ϕ_M is the macroporosity, b is a model parameter and **I** is the identity matrix. It is important to realize that in the double structure framework, the evolution of the clay fabric (macro and micro porosity) is controlled by the changes in the main variables of the problem (displacements, temperature, macro and micro suctions), which are considered in a fully coupled way. In this context, the main phenomena that affect the changes in both pores levels, and their mutual interactions, are taken into account. The limit condition of this thermo-hydro-mechanical model corresponds to the saturated state.

4. CONCLUDING REMARKS

Because of time constraints of experiments, it is unavoidable that the level of validation of a formulation and computer code will be much higher for the short initial transient period of an engineered barrier than for the barrier behaviour in the long term. Therefore, it is possible that formulations may require extensions and modifications even if they have been successfully validated for the short term.

Three phenomena have been identified as having a potential impact on the long term behaviour of engineered barriers: non Darcy-flow, thermo-osmosis and microfabric evolution. Effects of non-Darcy flow will only become apparent at low hydraulic gradients, precisely the situation expected at long times. Similarly, thermo-osmosis will only become significant when the advective flow due to hydraulic gradients fall to small values, again at long times, when the barrier is close to saturation. Thermo-osmosis effects will also depend on the magnitude of the thermal gradients at those times that, in turn, will depend on the specific design of the repository system. In addition, the effects of microfabric evolution will accumulate with time in step with the progress of saturation of the barrier. Therefore, the maximum difference (and the largest effect) with respect to the original microfabric will also be at the later hydration stages.

In this Deliverable the modifications of the conventional formulation required to incorporate those phenomena have been described in detail. Those modifications have been introduced and verified in the computer code CODE_BRIGHT and they are to be applied to a number of the analyses performed in the framework of the PEBS project.

ACKNOWLEDGMENT

The research leading to these results has received funding from the European Atomic Energy Community's Seventh Framework Programme (FP/7 2007-2011) under grant agreement 249681.

REFERENCES

Alonso, E., Gens, A. & Josa, A. (1990). "A constitutive model for partially saturated soils". *Géotechnique*, 40, 3, pp. 405-430.

Alonso, E., Vaunat, J. & Gens, A. (1999). "Modelling the mechanical behaviour of expansive clays". *Engineering Geology*, 54, pp. 173-183.

Batchelor, G:K: (1983). "Fluid Dynamics". *Cambridge University Press.*

Bear, J. (1972). "Dynamics of fluids in porous media". *Dover Edit.*, 164 pp.

CODE_BRIGHT User's Manual (2005). *UPC Geomechanical Group*.

Cui, Y., Loiseau, C. & Delage, P. (2001). "Water transfer through a confined heavily compacted swelling soil". *Proc. 6th International Workshop on Key Issues in Waste Isolation Research, Paris,* pp. 43-60

Djeran, I. (1993). "Étude des duffusions thermique et hydraulique dans una argile soumise á un champ de température". *Sciences et techniques nucléaires rapport*. Commission des Communautés européennes, ISBN 1018-5593.

Dixon, D., Gray, M. & Hatiw. (1992). "Critical gradients and pressures in dense swelling clays". *Can. Geotech. Jnl*., 29, pp. 1113-1119.

Dixon, D., Graham, J. & Gray, M. (1999). "Hydraulic conductivity of clays in confined tests under low hydraulic gradients". *Can. Geotech. Jnl*., 36, pp. 815-825.

FEBEX II Report (2004). "Final report on thermo-hydro-mechanical laboratory tests". Deliverable D17/3. UPC-L-7-13.

Gatabin, C. & Billaud, P. (2005). Bentonite THM mock up experiments. Sensors data report. CEA, Rapport NT-DPC/SCCME 05-300-A.

Gens, A. (2010). "Soil-environment interactions in geotechnical engineering. 47th Rankine Lecture". *Géotechnique*, 60, 3-74

Gens, A. (1995). "Constitutive Laws". In *Modern issues in non-saturated soils, A. Gens P. Jouanna & B. Schrefler (ed.)*: Wien New York: Springer-Verlag. pp. 129-158.

Gens, A. & Alonso, E.E. (1992). "A framework for the behaviour of unsaturated expansive clays". *Can. Geotech. Jnl*., 29, pp. 1013-1032.

Gens, A., Garcia Molina, A, Olivella, S., Alonso, E.E. & Huertas, F. (1998). "Analysis of a full scale in-situ test simulating repository conditions". *Int. Jnl. Numer. Anal. Meth. Geomech*, Vol. 22, pp. 515- 548.

Gens, A., Olivella, S. (2001). "THM phenomena in saturated and unsaturated porous media". Revue française de génie civil, 5: 693-717.

Hansbo, S. (1960). "Consolidation of clay with special reference to influence of vertical sand drains". *Swedish Geotech. Inst. Proc.* Nº 18 Stockholm.

Mitchell, J. (1993). "Fundamentals of soil behaviour". *2nd ed. John Wiley & Sons*, 437 pp.

Olivella., S. (1995). "Non isothermal multiphase flow of brine and gas through saline media". Ph.D. Thesis, Universitat Politecnica de Catalunya, UPC.

Olivella, S., Gens, A., Carrera, J. & Alonso, E.E. (1996). "Numerical formulation for a simulator (CODE-BRIGHT) for the coupled analysis of saline media". *Engineering Computations*, 13, 7, pp. 87-112.

Pollock, D.W. (1986). "Simulation of fluid flow and energy transport processes associated with high-level radioactive waste disposal in unsaturated alluvium". Water resource research Vol. 22 (5), pp. 765-775.

Pousada, E. (1984). “Deformabilidad de arcillas expansivas bajo succión controlada”. *PhD Thesis, Technical University of Madrid, Spain.*

Russell, A., & Swartzendruber, D. (1971). “Flux-gradient relationship for saturated flow of water through mixtures of sand, silt and clay”. *Sols Sci. Soc. Amer. Proc.* 35, pp. 21-26.

Sánchez, M. (2004). “Thermo-Hydro-Mechanical coupled analysis in low permeability media”. *PhD Thesis, Technical University of Catalonia, Spain*.

Sánchez, M.; Gens, A., Guimarães, L., & Olivella. S. (2005). “A double structure generalized plasticity model for expansive materials”. *International Journal for Numerical and Analytical Methods in Geomechanics,* 29: 751-787.

Sánchez, M., Gens, A., Olivella, S. (2012). “THM analysis of a large scale heating test incorporating material fabric changes” *International Journal Numerical and Analytical Methods in Geomechanics*, 36: 391-421

Soler, J.M. (1999). “Coupled transport phenomena in the opalinus clay: implications for radionuclide transport”. Paul Scherrer Institut Nº 99-07- ISSN 1019-0643.

Soler, J.M. (2001). “The effect of coupled transport phenomena in the Opalinus Clay and implications for radionuclide transport”. *Journal of Contaminant Hydrology* 53, 63–84.

Thomas, H. R., Cleall P. J., Chandler, N., Dixon, D. & Mitchell, H. P. (2003). Water infiltration into a large-scale in-situ experiment in an underground research laboratory. *Géotechnique*, 53, 207-224.

van Genuchten, R. (1978). “Calculating the unsaturated hydraulic permeability conductivity with a new closed-form analytical model”. *Water Resource Research*. 37(11), pp. 21-28.

Villar, M.V. & Cuevas, J. (1996). “Caracterización geoquímica de bentonite compactada. Efectos producidos por flujo termo-hidráulico”. *Informe Técnico 70 IMA-M-0-02.*